



**HAL**  
open science

## Propagation of a transverse wave on a foam microchannel

Caroline Derec, Valentin Leroy, Dimitri Kaurin, Louise Arbogast, Cyprien  
Gay, Florence Elias

► **To cite this version:**

Caroline Derec, Valentin Leroy, Dimitri Kaurin, Louise Arbogast, Cyprien Gay, et al.. Propagation of a transverse wave on a foam microchannel. 2015. hal-03256387v1

**HAL Id: hal-03256387**

**<https://hal.science/hal-03256387v1>**

Preprint submitted on 1 Aug 2015 (v1), last revised 20 Apr 2023 (v2)

**HAL** is a multi-disciplinary open access archive for the deposit and dissemination of scientific research documents, whether they are published or not. The documents may come from teaching and research institutions in France or abroad, or from public or private research centers.

L'archive ouverte pluridisciplinaire **HAL**, est destinée au dépôt et à la diffusion de documents scientifiques de niveau recherche, publiés ou non, émanant des établissements d'enseignement et de recherche français ou étrangers, des laboratoires publics ou privés.



Distributed under a Creative Commons Attribution 4.0 International License

# Propagation of a transverse wave on a foam microchannel

C. Derec<sup>1</sup>, V. Leroy<sup>1</sup>, D. Kaurin<sup>1</sup>, L. Arbogast<sup>1</sup>, C. Gay<sup>1</sup> and F. Elias<sup>1,2</sup>

<sup>1</sup> *Laboratoire Matière et Systèmes Complexes (MSC) - Université Paris-Diderot, CNRS UMR 7057, Paris, France.*

<sup>2</sup> *Sorbonne Universités, UPMC Université Paris 6, UFR 925 - Paris, France.*

In a foam, soap films meet by three in the liquid micro channels, called Plateau borders, which contain most of the liquid of the foam. We investigated here the transverse vibration of a single Plateau border isolated on a rigid frame. We measured and we computed numerically and analytically the propagation of a transverse pulse along the channel in the 20-2000 Hz frequency range. The dispersion relation shows different scaling regimes, which provide information on the role of inertial, elastic and viscous forces acting on the Plateau border: at low frequency, the dispersion relation is dominated by the vibration of the deformed soap films and the displacement of the surrounding air, and the Plateau border behaves as the free border of a soap film. The inertia of the liquid in the Plateau border plays a role at high frequency, the critical frequency separating the low frequency and the high frequency regimes being a decreasing function of the width  $R$  of the Plateau border.

## I. INTRODUCTION

Liquid foams are dispersions of gas bubbles in a liquid matrix stabilized by surfactants. Due to their diphasic nature, the macroscopic behavior of liquid foams is complex and closely linked to the structure of the liquid skeleton [1]. The acoustic propagation in liquid foams displays such a complex behavior: acoustic resonances and several regimes of propagation have been recently evidenced [2, 3], and interpreted as a result of the mechanical coupling between the constitutive elements of the foam skeleton: soap films, liquid channels and the air [3]. However, in order to model the acoustic propagation in a foam, systematic studies of this local coupling must be conducted to identify the local origin of inertia, elasticity and dissipation in a vibrating foam, and the relative roles of the physical characteristics of the bulk liquid, of the gas and of the gas-liquid interfaces.

The liquid network of a foam has a well-defined structure. The liquid is contained predominantly in the Plateau border (PB) channels, which form the edges of

the faces of the polyhedral bubbles (Fig. 1(a)): faces (soap films) meet threefold at 120 degrees in PBs. Each PB is terminated by two vertices in which four PBs meet tetrahedrally [1]. PBs can be isolated on rigid frames, and vibrated by an external forcing in order to study the foam vibration at the scale of the bubbles. Besson *et al.* [4] have studied the case of an annular PB at the junction between two adhesive bubbles; they have evidenced a frequency-dependent modulation of the contact angles between the bubbles during a periodical oscillation of the distances between the bubbles. Hutzler *et al.* [5] have considered the growth of a linear PB, freshly created during a topological rearrangement. They have observed a free oscillation of the length of the PB, and suggested that the frequency is fixed by the inertia of the displaced air, as described for example in [6]. However, no systematic study of the coupled vibration of a soap film connected to a PB has been performed yet.

Several works currently attempt to rationalize the coupled dynamics of the air, the soap films and the PB. These studies differ by the geometry investigated and by the amplitude of the forcing. Seiwert *et al.* investigate the case of an annular PB bounding a horizontal soap film suspended to two catenary films [7]. The free and forced oscillations of the PB and the connected soap film display a coupled dynamics where the displaced air plays a crucial role. In this configuration and in the frequency range investigated, the soap film retains a parabolic shape during the vibration. Cohen *et al.* [8] consider the case of a linear PB, transversally vibrated with a high forcing amplitude: they observe the modulation of the cross-sectional area of the PB in response to the vibration.

In this letter, we consider the propagation of a transverse wave along a linear PB. The PB is long enough so that several wavelengths take place along the PB. We measure the dispersion relation of the wave, for a small forcing amplitude. A numerical and analytical model of the wave propagation is developed and compared to the experimental data. Two regimes of propagation are evidenced in the frequency range 20-2000 Hz. At low frequency, the dynamics is dominated by the vibration of the adjacent soap films and the PB behaves as the free

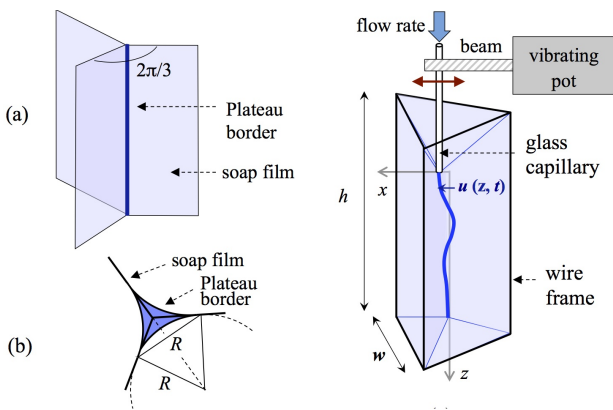


FIG. 1: (a) Sketch of a Plateau border at the junction between three soap films (side view). (b) Cross section (top view) of the PB at equilibrium:  $R$  is both the thickness and the radius of curvature of the PB. (c) Experimental setup (see description in the text).

border of the films. At high frequency or large PB radius, the inertia of the PB has to be taken into account. It increases the wave number and lowers the phase velocity of the wave.

## II. EXPERIMENTS

A single Plateau border is created by pulling a rigid plastic wire frame out of a soap solution. The frame (Zometool plastic struts and balls) is made of two horizontal equilateral triangles (width  $w = 20$  cm) linked at the vertices by vertical beams (height  $h = 23$  cm) as shown in Fig. 1c. In this geometry, three vertical soap films are formed and meet at the centre of the prism to form a PB. The soap solution is made of distilled water, commercial dishwashing liquid (Fairy Liquid, 1 vol. %) and glycerol (2 vol. %). The mass per unit volume of the solution is  $\rho_l = 1003$  kg m $^{-3}$  and the surface tension is  $\gamma = 30$  mN m $^{-1}$ . At equilibrium, the PB is straight and vertical, along the  $z$  axis. We insert into its top vertex the tip of a vertical glass capillary (Fig. 1c.). The capillary is connected to a vibrating pot, which generates a transverse controlled vibration along the horizontal  $x$  axis, in the plane of one of the three films meeting at the PB. As a result of capillary forces, the vertex remains attached to the capillary, and a transverse wave propagates along the PB in the  $z$  direction. The vertical  $z$  axis is the equilibrium position of the undeformed PB; the tip of the capillary defines the origin  $z = 0$ . The transverse displacement of the PB  $u(z, t)$  along the  $x$  direction is recorded using a high speed camera (Phantom V9) placed at a fixed adjustable height  $z$ , fitted with a high-magnification objective (Navitar Zoom 6000). Fig. 2 shows the variation of the displacement  $u(t)$  of the PB at different heights  $z$  during the propagation, where the incident pulse is a single undulation starting at  $t = 0$  and  $z = 0$ . The wire frame is large enough to postpone sufficiently the arrival of the reflected pulse coming from the soap boundaries or from the other end of the PB: we checked that the signals presented in Fig. 2 correspond to the incident propagating pulse alone. Soap solution can be injected at a constant flow rate  $Q$  through the capillary using a syringe pump (Pharmacia Biotech P500). The flow rate  $Q$  controls the PB radius  $R$ . We find that for  $Q < 3$  ml/min, the variation of  $R(z)$  is smaller than 10 % as soon as  $z > 2$  cm.[13] The average vertical velocity of the liquid flowing in the PB is  $V_z = Q/(CR^2)$  where  $CR^2$  is the section of the PB with  $C = \sqrt{3} - \pi/2 \simeq 0.161$  (Fig. 1b).  $V_z$  varies between 0.09 m/s and 0.17 m/s in the range of flow rates investigated here.

Fig. 2 shows the propagation of a transverse pulse along the PB. The first extremum of the signal propagates at a velocity of the order of 2 m s $^{-1}$ . However, the deformation of the signal when  $z$  increases shows that the propagation is dispersive. For a more precise analysis of the dispersion, we performed Fast Fourier Transform

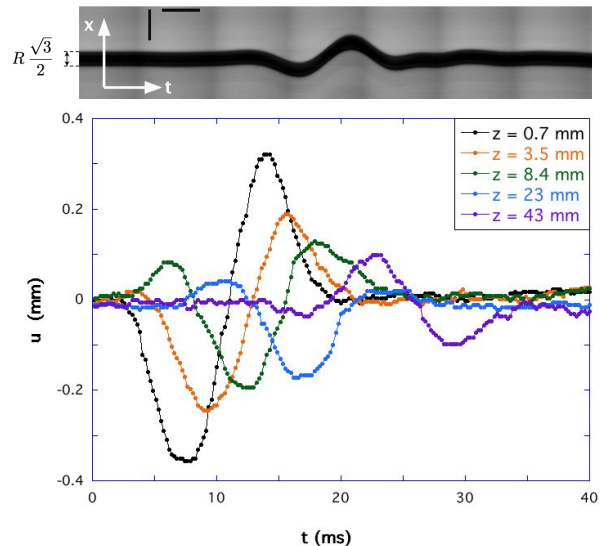


FIG. 2: Top: space-time diagram of the propagation of a transverse pulse along the Plateau border, for  $f_0 = 75$  Hz,  $Q = 2$  ml/min and  $z = 3$  cm,  $z = 0$  being the altitude of the exciting capillary. The Plateau border appears in black. The PB radius  $R$  is deduced from the thickness measurement. The vertical black bar represents 1 mm and the horizontal bar represents 5 ms. Bottom: propagation of the transverse pulse along the Plateau border each color corresponds to a different altitude below the capillary.

(FFT) of the temporal signal. The FFTs of two signals at two different heights  $z$  and  $z + \Delta z$ , are compared, and the phase shift  $\phi$  and the amplitude ratio  $T$  are extracted for each angular frequency  $\omega$ . Each mode of propagation of the transverse wave along the PB is written

$$u_q(t, z) = u_0 e^{i(\omega t - qz)}. \quad (1)$$

The real and imaginary parts of the complex wave number are then given by  $\Re(q) = \phi/\Delta z$  and  $\Im(q) = -\ln(T)/\Delta z$ . We checked that the measurements are independent of  $\Delta z$ , as soon as  $z > 2$  cm. Each signal allowed us to explore a given range of frequencies, around the central frequency of the pulse. Several acquisitions at different central frequencies were made to broaden the frequency range of the dispersion relation.

The imaginary part of the wave vector (not shown here) lies between 10 and 25 m $^{-1}$  in the whole investigated frequency range. This is at least one order of magnitude lower than  $\Re(q)$ , therefore  $\Im(q)$  will be neglected in the following, and the wave vector  $q \simeq \Re(q)$  is considered as a real number. The dispersion relation of the transverse wave along the PB is shown in Fig. 3. The parameters used in the experiments are shown in Table I. At low frequency or for small  $R$ , all the data collapse on the same master curve, described by a power law  $q \propto \omega^{2/3}$ . This law corresponds to the dispersion relation of a transverse wave on a soap film, and suggests that the PB behaves as the free border of a soap film. At higher frequency, and for the largest values of  $R$ , the data deviate from this

TABLE I: Values of the parameters used in the experiments. The flow rate  $Q$  is a control parameter. The radius  $R$  of the PB is determined using image analysis (see Fig. 2); the thickness  $e$  of the soap films is measured using a white light spectrometer (IDIL Fibres optiques – USB2000). The relative errors on  $R$  and on  $e$  are 10 %. The differences between several values of  $R$  for the same  $Q$  remain within errors, except for  $Q = 0$ , where the value of  $R$  depends on the time elapsed since the PB has been formed.

$Q$ (ml/min)	0	0	0	0	0.2	0.2
$R$ (mm)	0.03	0.04	0.07	0.12	0.18	0.19
$e$ ( $\mu\text{m}$ )	0.15	0.15	0.15	0.15	0.9	0.9
$Q$ (ml/min)	0.5	1	1	2	2	3
$R$ (mm)	0.27	0.41	0.44	0.53	0.60	0.72
$e$ ( $\mu\text{m}$ )	1.6	2.3	2.3	2.8	2.8	2.8

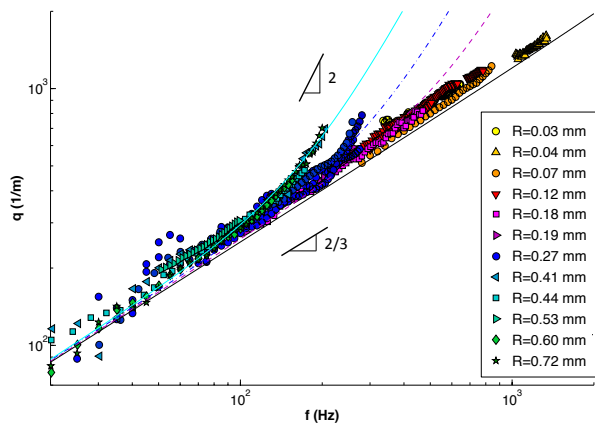


FIG. 3: Dispersion relation of the transverse wave on the PB for different radius  $R$ . The lines correspond to Eq. (15) without any fitting parameter. Black solid line:  $R = 0.03$  mm, magenta dotted line:  $R = 0.18$  mm, blue dashed line:  $R = 0.27$  mm and cyan solid line:  $R = 0.41$  mm. The typical power laws  $q \sim f^{2/3}$  and  $q \sim f^2$  are indicated on the graph.

power law; the larger the  $R$ , the smaller the frequency separating both regimes: In this regime, the inertia of the PB starts to play a role. Simultaneously, we observed that in this regime the amplitude of vibration suddenly decreases. Hence, only the start of this regime can be measured with our experimental technique.

### III. MODEL: PROBLEM STATEMENT

The PB is the meeting line between three soap films. The vibration occurs along the  $x$  direction, in the plane of one soap film, and causes an out-of-plane vibration of the other two films called film 1 and film 2 (see Fig. 4a). Let  $(y_1, z)$  be the plane of film 1, and  $x_1$  the axis normal to this plane, which forms an angle of  $\pi/3$  with the  $x$  axis (Fig. 4). Similarly,  $(y_2, z)$  is the plane of film 2, and  $x_2$  the axis normal to this plane.  $(x_1, y_1, z)$  and  $(x_2, y_2, z)$  define two direct orthonormal frames, tilted one with re-

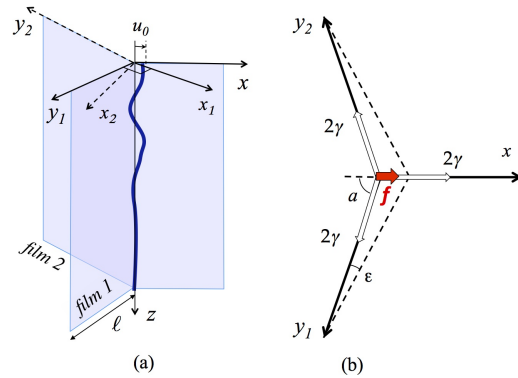


FIG. 4: (a) Side view of the PB and notations (see text). (b) Top view of the three soap films meeting at the PB. The dashed lines correspond to the PB at equilibrium; the solid lines correspond to the deformed PB. Each soap film pulls on the PB with a force per unit surface equal to  $2\gamma$ .

spect to another so that the three axes  $x$ ,  $x_1$  and  $-x_2$  form relative angles of  $\pi/3$ . The transverse displacements of film 1 and film 2 along  $x_1$  and  $x_2$  are respectively denoted by  $\zeta_1$  and  $\zeta_2$ . Since  $(x, z)$  is a plane of symmetry of the system,  $\zeta_2(y_2, z) = -\zeta_1(y_1, z)$  when  $y_2 = y_1$ . In the following, we describe the deformation of film 1.

The transverse deformation of film 1 and film 2 leads locally to a deviation from  $2\pi/3$  of the angles at the PB. Therefore, a net restoring force  $\vec{f}$  due to the surface tension acts on the PB to bring it back to equilibrium (Fig. 4b) [9]. Moreover, the transverse vibration of the films causes a displacement of the surrounding air [6, 10]. Therefore, the propagation of the transverse wave on the PB results from the coupling between the vibration of the PB, of the films and of the surrounding air.

Three main simplifications are assumed in the following model. First, the role of the longitudinal deformations of the films is neglected and only the transverse deformations are considered. It means that the films are infinitely compressible, with an instantaneous response. In other words, the role of the interfacial visco-elasticity is neglected compared to the role of the surface tension forces. Second, we assume that the problem is linear, therefore the Fourier modes are not coupled. Third, we consider that the soap film has an effective moving mass which takes into account the mass of liquid and the mass of the displaced surrounding air, according to the dispersion relation of an infinite soap film [10]. This assumption is valid for a periodic oscillation [14]. The model developed below thus describes the propagation of a single mode of oscillation. Finally, the amplitude of the deformation remains small compared to the wavelength. Under these assumptions, the dispersion relation can be computed as follows.

Considering  $\zeta_1(y_1, z, t) = \zeta_1(y_1, z)e^{i\omega t}$ , the equation of the transverse motion of soap film 1 writes:

$$m_f \ddot{\zeta}_1 = 2\gamma (\partial_{y_1}^2 + \partial_z^2) \zeta_1 \quad (2)$$

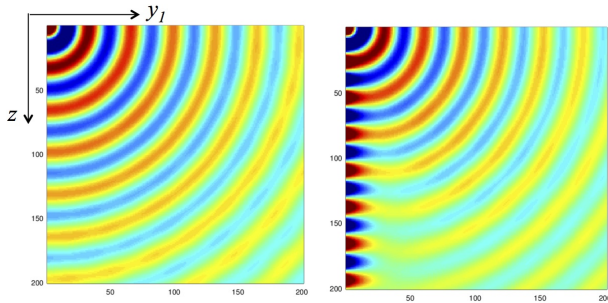


FIG. 5: Numerical resolution of Eqs. (5) and (6) with  $f = 200$  Hz,  $N_y = N_z = 800$  and  $d_y = d_z = 0.5$  mm (displayed region is  $n_y, n_z \leq 200$ ). Left:  $R = 0.03$  mm *i.e.*  $\alpha/k = 0.006$ ; right:  $R = 0.27$  mm *i.e.*  $\alpha/k = 0.43$ .

where  $m_t = m_t(\omega)$  is the effective mass per unit surface area of the film (see below). The restoring force  $\vec{f}$  exerted by the soap films pulling on the PB is along the  $x$  axis (fig. 4b) and its amplitude is  $f = 2\gamma(1 - 2\cos a) = 2\gamma[1 - 2\cos(\pi/3 + \varepsilon)] \simeq 2\sqrt{3}\gamma\varepsilon$  in the limit of small deformations, where  $2a$  is the relative angle between film 1 and film 2, and  $\varepsilon$  is the local deviation of film 1 from equilibrium:  $\varepsilon = \partial_{y_1}\zeta_1(y_1 = 0)$  [9]. The inertia of the PB is of the form  $\mu(\partial_t + V_z\partial_z)\partial_t u$ , where  $\mu = \mathcal{C}\rho_1 R^2$  is the linear mass of the PB and  $V_z$  is the average vertical liquid velocity in the PB. Considering a single mode of propagation (Eq. (1)), the inertia becomes  $-\mu\omega(\omega - qV_z)$ . In the experiments,  $V_z$  is 10 to 50 times smaller than  $\omega/q$ , hence  $V_z$  will be neglected in the following. Therefore, the equation of the transverse motion of the PB reads:

$$\mu \ddot{u} = 2\sqrt{3}\gamma \partial_{y_1}\zeta_1|_{y_1=0}. \quad (3)$$

Since the PB lies at the edge  $y_1 = 0$  of the soap film, the following boundary condition must be satisfied:

$$\zeta_1(y_1 = 0, z, t) = \frac{\sqrt{3}}{2}u(z, t). \quad (4)$$

Eqs. (2) and (3) are the two equations of motion of the system. They are solved below considering a continuous forcing in  $z = 0$ :  $u(0, t) = u_0 e^{i\omega t}$ . They must be complemented with suitable boundary conditions to reflect the exact geometry of the forcing. Solving the whole system analytically requires some assumptions concerning the geometry of wave (plane or circular) propagating on the soap film. Because the forcing by the capillary is almost point-like, it should generate a circular wave on an infinite soap film. Here, the presence of an inertial PB at the edge of the film deforms the wave front. Therefore no simple approximation can be inferred concerning the geometry of the wave front. Consequently, we first compute numerically the solutions of Eqs. (2) and (3).

#### IV. NUMERICAL SIMULATIONS

Soap film 1 is approximated by a rectangle and discretized in directions  $y_1$  and  $z$  with  $N_y$  and  $N_z$  in-

tervals of length  $d_y$  and  $d_z$  respectively. The transverse displacement is represented by a complex amplitude,  $\zeta_1(y_1, z, t) = \zeta_0 A_{n_y, n_z} e^{i\omega t}$ , where  $y_1 = n_y d_y$  and  $z = n_z d_z$ , with  $0 \leq n_y \leq N_y$  and  $0 \leq n_z \leq N_z$ .

The imposed motion of the capillary is taken into account by setting a unit amplitude  $A_{0,0} = A_{0,1} = 1$ . Below the capillary, the PB sits at the boundary node  $n_y = 0$  at every altitude  $z = n_z d_z$  for  $n_z > 1$ .

The upper boundary at  $n_z = 0$  is assumed to be a free boundary, *i.e.* with a vanishing film slope  $\partial_z \zeta_1|_{z=0} = 0$ , which can be expressed as  $A_{n_y,1} - A_{n_y,0} = 0$ , or more precisely  $-\frac{3}{2}A_{n_y,0} + 2A_{n_y,1} - \frac{1}{2}A_{n_y,2} = 0$ , for all  $n_y > 0$ .

Eq. (2) translates into:

$$\frac{A_{n_y-1, n_z} + A_{n_y+1, n_z}}{d_y^2} + \frac{A_{n_y, n_z-1} + A_{n_y, n_z+1}}{d_z^2} + \left[ k^2 - \frac{2}{d_y^2} - \frac{2}{d_z^2} \right] A_{n_y, n_z} = 0 \quad (5)$$

with  $k^2 = \omega^2 m_f / (2\gamma)$ , and Eq. (3) into  $\alpha A|_{y_1=0} = \partial_{y_1} A|_{y_1=0}$ , which becomes:

$$\left( \alpha - \frac{3}{2d_y} \right) A_{0, n_z} + \frac{2}{d_y} A_{1, n_z} - \frac{1}{2d_y} A_{2, n_z} = 0 \quad (6)$$

with  $\alpha = \mu\omega^2 / (3\gamma)$ . The parameter  $\alpha$  comes directly from the first term of the left-hand part of Eq. (3). It depends on the section of the PB and on the frequency: this term controls the inertia of the PB. Similarly, the parameter  $k^2$  describes the inertia of the soap film. The results of the computation, conducted using free software GNU octave, are shown in Fig. 5 for two values of  $\alpha$ .

In the simulations, the forcing is a continuous oscillation. To minimize wave reflections at the edges of the film, we included an imaginary part  $k_d$  of  $k$  as described in ref. [10] to reflect the viscous dissipation in the air. We also took large samples (Fig 5 shows a region of size  $200 \times 200$  points out of  $800 \times 800$ ). At the remote edges ( $n_y = N_y$  and  $n_z = N_z$ ), we chose a fixed (vanishing) displacement, *i.e.*  $A = 0$ . Although  $k_d/|k| \ll 1$ , we checked that these boundary conditions do not to affect the system substantially in the region of interest.

Because the forcing is different in the numerical simulations (continuous oscillation) and in the experiments (single burst), the exact value of the transverse amplitude cannot be compared. However, the numerical calculation can be used to visualize the mapping of the deformation in the film. Fig. 5 shows that, for  $\alpha = 0$  (the edge of the film is free), the wave fronts are circular, as expected for a quasi-punctual perturbation. For  $\alpha \neq 0$ , the circular pattern is deformed close to the PB: a second wave pattern appears, confined along the PB, when the inertia of the PB is finite. In the following, we shall consider that the transverse deformation of the soap film is a linear superposition of a circular wave and of a plane wave localized close to the PB. Under those conditions, an analytical model can be derived.

## V. ANALYTICAL MODEL

In this section, we solve analytically Eqs. (2) and (3) considering the propagation of a single mode given by Eq. (1) on the PB. We consider two kinds of waves propagating on the soap film: a circular wave and a plane wave.

### A. Circular wave

Eq. (3) writes, in polar coordinates

$$\mu \ddot{u} = 2\sqrt{3}\gamma \frac{1}{r} \partial_\theta \zeta_1 |_{\theta=\pi/2} \quad (7)$$

where  $r$  is the radial distance from the tip of the capillary, and  $\theta$  is the polar angle from the  $y_1$  axis. In the case of a circular wave, the deformation  $\zeta_1(r, \theta, t)$  is radial, therefore  $\partial_\theta \zeta_1 = 0$ , and consequently  $\mu \ddot{u} = 0$ : only in the case of an infinitely thin PB or of a vanishing frequency the wave propagating in the soap film remains circular. If  $\mu \ddot{u} \neq 0$ , the presence of the PB must deform a circular wave in the vicinity of the PB, as illustrated in Fig. 5.

### B. Plane wave

We assume here a plane wave propagating in the soap film and along the PB:

$$\zeta_1(y_1, z, t) = \zeta_0 e^{i(\omega t - q_{y_1} y_1 - q_z z)} \quad (8)$$

where  $q_{y_1}$  and  $q_z$  are the components of the wave vector in the soap film. Using Eq. (8), Eqs. (4) and (1) lead to  $q = q_z$  and  $\zeta_0 = (\sqrt{3}/2)u_0$  and Eqs. (2) and (3) lead to:

$$\frac{m_f}{2\gamma} \omega^2 - q_{y_1}^2 - q^2 = 0 \quad \text{and} \quad \frac{\mu}{3\gamma} \omega^2 = i q_{y_1}. \quad (9)$$

Therefore:

$$q^2 = \frac{m_f}{2\gamma} \omega^2 + \left(\frac{\mu}{3\gamma}\right)^2 \omega^4. \quad (10)$$

Eqs (9) and (10) can be simplified:

$$\begin{aligned} q_{y_1} &= -i\alpha \\ q^2 &= k^2 + \alpha^2, \end{aligned} \quad (11)$$

where  $\alpha$ , and  $k$  are defined after Eq. (6). Fig. 6a shows that the amplitude of the transverse displacement decreases exponentially in the  $y_1$  direction of the soap film, with a decreasing rate equal to  $\alpha$ , as predicted by Eq. (11). Eq. (12) gives the (implicit, see below) dispersion relation of a transverse plane wave on the PB. It is plotted in Fig. 6b, which shows that the data extracted from the numerical simulations, performed with  $d_y = d_z = 0.5\text{mm}$  (circles),  $0.2\text{mm}$  (squares) and  $0.1\text{mm}$  (triangles), are very well described by the Eq. (12).

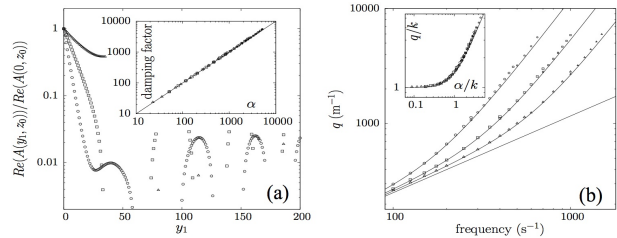


FIG. 6: Comparison between the numerical and the analytical dispersion relation, for  $R = 0.18$  mm (triangles),  $R = 0.27$  mm (squares) and  $R = 0.41$  mm (circles). (a) Amplitude of the transverse displacement in the  $y_1$  direction. The amplitude decreases exponentially, with a damping factor equal to  $\alpha$  (insert), as predicted by Eq. (11). (b) Wavenumber  $q$  given by the numerical simulations (dots) and by Eq. (10) with  $\mu = C\rho_l R^2$  (solid lines) as a function of  $f$ . Insert: master curve displaying  $q/k$  versus  $\alpha/k$  in numerical simulations (dots) and according to Eq. (12) (solid line).

Those comparisons validate the analytical model of a localized plane wave propagating along the PB. Therefore, this analytical model is used in the following to describe the experimental data.

## VI. COMPARISON BETWEEN THE MODEL AND THE EXPERIMENTAL DATA

In order to be compared to the experimental dispersion relation presented in Fig. 3, Eq. (12) must be expressed as a function of measurable parameters. The effective displaced mass per unit surface area  $m_f = m_f(\omega)$  is implicitly given by the dispersion relation of a transverse wave on an infinite soap film [10]:

$$\frac{\omega^2}{k^2} = \frac{2\gamma}{m_f} = \frac{2\gamma}{\rho_l e + 2\rho_a/k}. \quad (13)$$

where  $k(\omega)$  is the real part of the wave number of the transverse wave on the soap film and  $\rho_a = 1.2 \text{ kg m}^{-3}$  is the mass per unit volume of the surrounding air. We introduce the notations  $k_0 = (\rho_a \omega^2 / \gamma)^{1/3}$  and  $\delta = \rho_l e / (6\rho_a)$ . Eq. (13) reads  $k^3/k_0^3 = 1 + 3k\delta$  and has one real positive solution:

$$k/k_0 = \left[ \frac{1 + \sqrt{1 - 4(k_0\delta)^3}}{2} \right]^{1/3} + \left[ \frac{1 - \sqrt{1 - 4(k_0\delta)^3}}{2} \right]^{1/3}. \quad (14)$$

In our experimental conditions,  $k_0\delta \ll 1$  and Eq. (14) can be developed to the first order in  $k_0\delta$ . Therefore, eq. (12) becomes  $q \simeq \sqrt{k_0^2 + 2k_0^3\delta + \alpha^2}$ , that is:

$$q \simeq \sqrt{\left(\frac{\rho_a}{\gamma}\right)^{2/3} \omega^{4/3} + \frac{\rho_l e}{3\gamma} \omega^2 + \left(\frac{\rho_l C R^2}{3\gamma}\right)^2 \omega^4}. \quad (15)$$

The comparison between Eq. (15) and the experimental data is shown in Fig. 3. The data are very well described by the analytical dispersion relation without any fitting

parameter. The low frequency or small  $R$  regime is described by a power law  $q \simeq k_0 \propto \omega^{2/3}$ . In this regime, the dispersion relation of the PB is the same as the dispersion relation of transverse waves on a soap film, the inertia being dominated by the displaced air: the PB behaves as the free border of a vibrating soap film. When the frequency or the PB radius increases, the inertia of the liquid in the PB affects the vibration of the soap film edge. Asymptotically, the high frequency or large  $R$  regime is dominated by the inertia of the liquid in the PB, according to Eq. (15):  $q \simeq \alpha \propto R^2 \omega^2$ . We do not capture this asymptotic regime experimentally because of the sudden decrease of the amplitude of vibration of the PB at high frequency. However we clearly observe a crossover between the low frequency  $q \propto \omega^{2/3}$  behavior and another regime with a higher exponent at higher frequencies, and the crossover frequency is lower for higher  $R$ .

## VII. DISCUSSION AND CONCLUSION

By mixing experiments, numerical and analytical analysis, we have shown that the propagation of a transverse displacement wave along a linear vertical PB isolated on a frame exhibits two regimes of propagation, in the range 20 Hz - 2000 Hz: a low-frequency regime, dominated by the vibration of the adjacent soap films, and a high-frequency regime, where the inertia of the PB dominates. The frequency of transition between those two regimes is a decreasing function of the PB cross-section.

Several points have to be discussed. Firstly, the vertical liquid velocity has been neglected here. This liquid advection should decrease  $q$  and have larger effect for the larger flow rate. It might explain that in Fig. 3, the data corresponding to the highest  $R$  seem to saturate, and have a value lower than expected.

Secondly, the vanishing vibration amplitude, which limits the accessible frequency range at high frequency or large PB is not fully understood. We suspect that it could be due to a low transmission in the intermediate region between the end of the capillary and the PB: in this region, the PB is strongly deformed along a length  $L_t$  over which it transits from a positive to a constant negative curvature. If  $L_t$  is larger than some attenuation length  $L_a$ , the signal would be totally damped in the PB.  $L_t$  should increase with the liquid flow rate  $Q$  and  $L_a$  should decrease with an increasing frequency  $f$ ; therefore the signal could be totally damped if  $Q$  is large enough (*i.e.* for large  $R$ ) or if  $f$  is large. However, rationalization of the dissipation in the transient region would be necessary for a complete understanding of this effect, which is beyond the scope of the present letter.

Finally, the attenuation of the signal along the PB is too small to be measurable with the technique presented here. In the future, we plan to investigate the resonances curves of the vibrating wave on the PB as a function of the frequency, to measure the imaginary part of the wave vector of the PB. Changing the physicochemical composition of the surfactant solution and of the gas should allow us to systematically describe the contributions of the dissipation in the bulk liquid, in the deformable interfaces and in the gas. We believe that this study could bring new elements to address the more general problem of the dissipation in liquid foams, which is an important and currently active subject of research (see for example the reviews [11, 12] and references therein).

We acknowledge funding support from the Agence Nationale de la Recherche (ANR-11-BS09-001) We thank B. Dollet, C. Raufaste, A. Cohen, W. Drenckhan, J.-C. Bacri and F. Graner for fruitful discussions.

- 
- [1] Cantat I., Cohen-Addad S., Elias F., Graner F., Hohler, Pitois O., Rouyer F. & Saint-Jalmes A., *Foams. Structure and Dynamics*, Edited by S. Cox (Oxford University Press) 2013
  - [2] Ben Salem I., Guillermic R. M., Sample C., Leroy V., Saint-Jalmes A. & Dollet B. *Soft Matter*, 9 (2013) 1194.
  - [3] Pierre J., Dollet B. & Leroy V. *Phys. Rev. Lett.* 112 (2014) 148307.
  - [4] Besson S. & Debregeas G. *Eur. Phys. J. E* 24 (2007) 109-117.
  - [5] Hutzler S., Saadatfar M., van der Net A., Weaire D. & Cox S. J. *Coll. Surf. A*. 323 (2008) 123-131.
  - [6] Afenchenko V. O., Ezersky A. B., Kiyashko S. V., Rabinovich M. I. & Weidman P. D. *Phys. Fluids*.10 (1998) 390.
  - [7] Seiwert J., Pierre J. & Dollet B. *submitted*.
  - [8] Cohen A., Fraysse N. & Raufaste C. *in preparation*.
  - [9] Elias F., Janiaud E., Bacri J.-C. & Andreotti B. *Phys. Fluids* 26 (2014) 037101.
  - [10] Kosgodagan Acharige S., Elias F. & Derec C. *Soft Matter* 10 (2014) 8341.
  - [11] Dollet B. & Raufaste C. *C. R. Physique* 15 (2014) 731.
  - [12] Cohen-Addad S. & Hohler R. *Curr. Opin. Colloid Interface Sci.*19 (2014) 536.
  - [13] An expression for  $R(Q, z)$  was derived in ref. [9]. Here,  $R(Q)$  is compatible with a Poiseuille law with mobile interfaces:  $R \simeq [\mathcal{D}\nu Q/(Cg)]^{1/4}$  where  $\mathcal{C} \simeq 0.161$ ,  $\nu$  is the kinematic viscosity of the liquid and  $\mathcal{D}$  is linked to the interfacial mobility (here  $\mathcal{D} \simeq 2.9$ ).
  - [14] For an arbitrary deformation, the effect of the displaced air would result in non-local interactions within the film, both in space and time.